Kim, Y.E., *Surface reaction mechanism for deuterium-deuterium fusion with a gas/solid-state fusion device.* Fusion Technol., 1991. **19**: p. 558.

SURFACE REACTION MECHANISM FOR DEUTERIUM-DEUTERIUM FUSION WITH GAS/SOLID-STATE FUSION DEVICE

Yeong E. Kim
Department of Physics
Purdue University
W. Lafayette, Indiana 47907, U.S.A.

Abstract

Recent highly reproducible results of tritium production by deuterium-deuterium (D-D) fusion from gas/solid-state fusion experiments are discussed in terms of a surface fusion mechanism. Theoretical criteria and experimental conditions for improving and optimizing D-D fusion rates in a gas/solid-state fusion device are described. It is shown that the surface fusion mechanism also provides a plausible explanation for the nonreproducibility of the results of electrolysis fusion experiments.

I. INTRODUCTION

Recently, a surface fusion mechanism[1,2] was proposed to explain the discrepancy of 24 to 60 orders of magnitude between claimed results of electrolysis fusion experiments[3-18] and the conventional estimates[19-21] for deuterium-deuterium (D-D) fusion. The effect of a velocity distribution[22] in the context of the surface fusion mechanism was shown to be very important in reducing this discrepancy. More recently, it has been suggested[23] and shown[24] that the effect of electron screening becomes significant at low energies and further reduces the discrepancy. However, the claimed positive results[3-18] of electrolysis fusion experiments are not yet reproducible. Furthermore, there are also many negative results[25-28] of electrolysis experiments.

Claytor *et al.*[29] have been investigating D-D fusion processes in a nonelectrolytic gas/solid-state (G/S) device and have succeeded in attaining reproducible results for tritium production from their G/S cells. In this technical note, the experimental results of Claytor *et al.*[29] are explained in terms of the surface fusion mechanism.[1,2,22-24] Theoretical criteria and experimental conditions for improving and optimizing the D-D fusion rates in the G/S fusion devices are described in the context of the surface fusion mechanism.[1,2,22-24] It is also shown that the surface fusion mechanism provides a plausible explanation for the nonreproducibility of results of electrolysis fusion experiments.[3-18,25-28]

In section II, D-D fusion reactions are described in terms of the surface fusion mechanism as they relate to a G/S fusion device and the results of Claytor *et al.*[29] and effects of electron screening and velocity distribution on D-D fusion rates are discussed. The observed anomalous branching ratio for D-D fusion reactions is also discussed in this section. In section III, theoretical criteria and experimental conditions for improving and optimizing the D-D fusion

rates in a G/S fusion device are given in the context of the surface fusion mechanism. Finally, a brief summary and conclusions are given in section IV.

II. SURFACE FUSION MECHANISM

The G/S fusion cells used by Claytor *et al.*[29] were constructed of alternating layers of palladium and silicon powders pressed into a ceramic disc stack and exposed to D_2 gas at 110 psi resulting in a D/Pd ratio of 0.7. Pulsed dc voltages were applied to pass pulses of current through cells, which are kept in the pressurized D_2 gas at an operating temperature near the ambient temperature. The pulses used were of 1 μs to 1 ms in duration at voltages up to 3000 V and at currents as high as 0.5 ampere with a low duty cycle (~ 10 ms) to reduce Joule heating. Since the palladium and silicon layers are made of pressed powders, there are numerous ($\gtrsim 10^6$) D_2 gas pockets of ~ 10 μm size distributed throughout these layers and at the interfaces between the layers.[29] In several runs of 60- to 90-h duration, they observed a tritium production rate of $R^T_{\rm exp} \approx 10^7$ s^{-1} and a neutron production rate of $R^n_{\rm exp} \approx 10^{-2}$ s^{-1} corresponding to a branching ratio of $R^T_{\rm exp} / R^n_{\rm exp} \approx 10^9$. More importantly, their results seem to be highly reproducible.[29]

In the surface fusion mechanism,[1,2] an electric field is generated in each of the D_2 gas bubbles (in an electrolysis experiment) or pockets (in a G/S fusion device) on the surface of the deuterated metal (palladium cathode or layer) due to an applied external voltage, as shown in Fig. 1. This electric field accelerates positively charged deuterium ions (D^+ and D_2^+) which are produced by ionization and dissociation of D_2 molecules in the D_2 gas. These deuterium discharge currents are incident on deuterium embedded in the deuterated metal or on deuterium in the D_2 gas, which acts as the deuteron target.

In a typical electrolysis experiment, there are several possible mechanisms which can accelerate deuterium ions through D_2 gas bubbles or through a D_2 gas layer which has formed on the surface of the cathode. Due to the isobaric hysteresis[30] of deuterium solubility in palladium as a function of the palladium temperature, D_2 gas bubbles can be produced rapidly and uniformly on the palladium surface during hysteresis, and can virtually cover the palladium cathode. Because of instability and difficulty of creating and maintaining a thin D_2 gas layer, it is difficult to achieve and reproduce the same result with same and/or similar electrolysis cells. Although the potential difference across a given D_2 gas bubble is expected to be a fraction of the applied potential across the electrolysis cell, Rabinowitz and Worledge[31] have suggested several nonequilibrium situations in which high potential differences can occur:

1. Gas bubbles of H_2/D_2 can form into a layer that virtually covers the palladium cathode, thereby allowing the formation of a high double-layer electric field which is enhanced at the sharp tips of surface asperities (or whiskers); this electric field can be ~ 10^9 V/m along with a high D^+ current, even though the voltage across the electrolysis cell is only ~ 1 V.

2. The breaking of direct contact between the electrolyte solution and small regions on the surface of the cathode by the interposition of accumulating D_2 gas bubbles leads to the possibility for breakdown arcing across these bubbles with attendant huge spark discharge current densities ($\lesssim 10^5$ A/cm^2) (Refs. 32 and 33); this would be especially true with the presence of asperities.

3. A small number of deuterons can become entrained with high current density electrons. Even though these electrons can have energies only of the order of ~ 10 eV, the entrained D^+ can

obtain energies ~ 37 keV, since the ratio of the deuteron energy to electron energy would be $(M_D v^2/2)/(M_e v^2/2) = M_D/M_e \approx 3670$. Because of the different sizes of the D_2 gas pockets and different values of the widely varying electric field inside each pocket, D^+ ions will gain kinetic energies with a statistical velocity distribution.

The possibility of a high double-layer field with surface asperities has been also suggested by Lin *et al.*[34] A different model of the surface double layer has been proposed by Hora *et al.*[35] An alternative explanation for the nonreproducibility of the results of electrolysis experiments has been proposed by Handel[36] based on difficulties of achieving homogeneous nucleation of D_2 bubbles on the surface of the cathode.

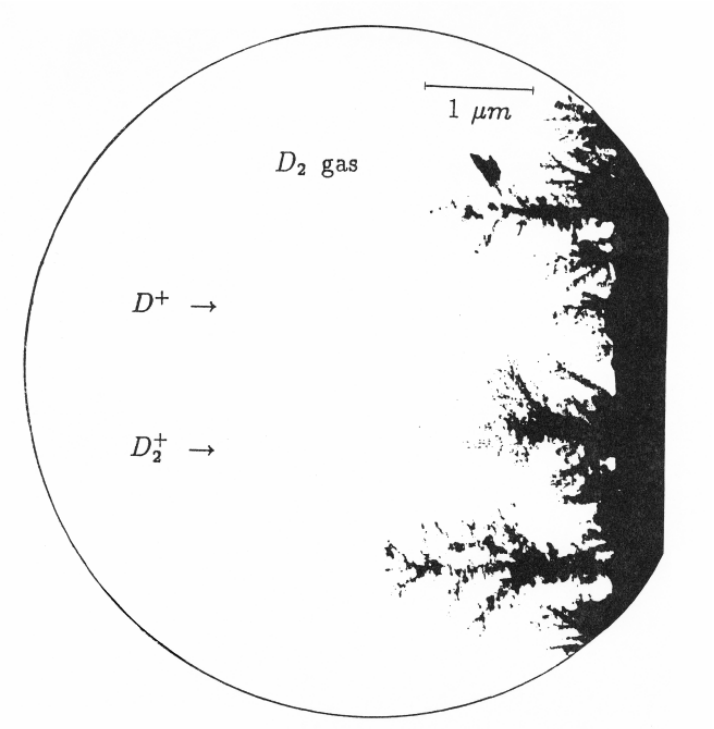

Fig. 1. Schematic picture of a D_2 gas pocket (or bubble) which acts as a micro surface-fusion chamber. The dark area represents the palladium surface with whiskers. The solid line represents the surface of the D_2 gas pocket.

II.A Fusion Reaction Cross-Sections

In the G/S fusion experiment,[29] the dominant fusion reactions are expected to be

$$D^+ + D \rightarrow {}^3H\ (1.01\ \text{MeV}) + p(3.02\ \text{MeV}), \tag{1a}$$

and

$$D^+ + D \rightarrow {}^3He\ (0.82\ \text{MeV}) + n(2.45\ \text{MeV}). \tag{1b}$$

Experimental values of the cross-section, $\sigma(E)$, for (1a) and (1b) have been conventionally parameterized as[37]

$$\sigma(E) = \frac{S(E)}{E}\exp\left[-(E_G/E)^{1/2}\right] \tag{2}$$

where E_G is the "Gamow energy" given by $E_G = (2\pi\alpha Z_D Z_D)^2 Mc^2/2$ or $E_G^{1/2} \approx 31.39\ (\text{keV})^{1/2}$ for the reduced mass $M \approx M_D/2$ for reactions (1a) and (1b). E is in units of kilo-electron-volts in the center of mass (CM) reference frame. The S factor, $S(E)$, is extracted from experimentally measured values[38] of the cross-section, $\sigma(E)$, for $E \geq 4$ keV and is nearly constant,[39] $S(E) \approx 52.9$ keV – b, for both reactions (1a) and (1b) in the energy range of interest here, $E \leq 1$ keV.

The expression for $\sigma(E)$ given by Eq. (2) is valid only for a reaction in which D^+ is incident on another D+. In cold fusion experiments, D^+ is incident on deuterium which is shielded by an electron cloud; i.e., the target deuterium is electrically neutral outside the electron shielding radius (≤ 0.53 Å, the Bohr radius). Therefore, the Coulomb barrier penetration factor ("Gamow factor") in Eq. (2),

$$P_G(E) = \exp\left[-(E_G/E)^{1/2}\right], \tag{3}$$

which is appropriate only for the $D^+ + D^+$ reaction has to be modified for the case of the $D^+ + D$ reactions (1a) and (1b). The new modified barrier penetration factor appropriate for reactions (1a), (1b), and other fusion reactions is[23]

$$P_s(E) = \exp\left\{-E_G^{1/2}/\left[E + E_s(E)\right]^{1/2}\right\}. \tag{4}$$

We will discuss the derivation of this formula in Sect. II.B. When there is no electron screening, $E_s(E)$ vanishes, and we recover the conventional Gamow factor, $P_s(E) = P_G(E)$. Using Eq. (4), the new extrapolation formula appropriate for reactions (1a) and (1b) and other charged particle fusion reactions is

$$\sigma_s(E) = \frac{S(E)}{E}\exp\left(-\left\{E_G/\left[E + E_s(E)\right]^{1/2}\right\}\right). \tag{5}$$

The screening energy term $E_s(E)$ in Eq. (5) can be extracted from the measured values of $\sigma_{exp}(E)$ at very low energies for the D-D fusion reaction (1a) or can be uniquely calculated for a given electron screening potential.[23] The parameterization[37,39] of $S(E)$ used in Eq. (2) can also be used in Eq. (5), since $S(E)$ is determined from the measured cross-sections at higher energies $E >> E_s(E)$.

II.B Electron Screening Effect

With the presence of the electron screening potential, $V_s(r)$, the resultant modified Coulomb barrier penetration factor in the Wentzel-Kramers-Brillouin (WKB) approximation is

$$P_s(E) = \exp\left\{-2\left(\frac{2M}{\hbar^2}\right)^{1/2}\int_{r_N}^{r_a}\left[V_c(r) + V_s(r) - E\right]^{1/2} dr\right\} \tag{6}$$

where $V_c(r) = Z_i Z_t e^2/r$, r_N is the effective nuclear interaction range, and the classical turning point r_a is determined by $V_c(r_a) + V_s(r_a) = E$. Z_i and Z_t are the charges (in units of E) of the incident and target particles, respectively. The integral in Eq. (6), even for $r_N = 0$, which is an accurate approximation, cannot be carried out analytically in most cases. However, the numerical values of $P_s(E)$ obtained by numerical integration can be expressed by Eq. (4) for an attractive potential $V_s(r) < 0$. From Eqs. (4) and (6), it can be easily shown that $E_s(E)$ in Eq. (4) is bounded by $|V_s(r_a)| < E_s(E) < |V_s(0)|$. As an example, the electron screening potential for the deuterium

target atom generated from the 1*s* hydrogen electron density as seen by an incident deuteron is given by

$$V_s(r) = -\frac{Z_i Z_t e^2}{r}\left[1 - \exp(-ur)(1 + ur/2)\right], \tag{7}$$

Where

$u = 2/a_0$

$a_0 \approx 0.53$ Å, the Bohr radius.

The value $V_s(r)$ approaches $-Z_i Z_t e^2/r$ as $r \to \infty$, as expected. Value $V_s(r)$ is negative for $r \geq 0$ and $|V_s(r)|$ has a maximum value of $|V_s(0)| = Z_i Z_t e^2/a_0 = 27.17\, Z_i Z_t$ eV at $r = 0$. Since $|V_s(r)|$ decreases monotonically as r increases, $E_s(E)$ satisfies $E_s(E) \leq |V_s(0)|$. Thus, at the classical turning point of $r = r_a = a_0$ corresponding to $E = 7.35$ eV, $|V_s(a_0)| = 19.8 Z_i Z_t$ eV, and hence $E_s(E)$ is bounded by $27.17\ Z_i Z_t$ eV $> E_s(E) > 19.8\ Z_i Z_t$ eV.

The electron screening effect has definitely been detected in heavier reaction species[40,41] and the extracted values of $E_s(E)$ are found to be 66, 120, 210 and 300 eV for D(^{3}He$^+$, *p*)^{4}He (Ref. 40), ^{3}He(D$^+$, p)^{4}He (Ref. 40), ^{7}Li(*p*,^{4}He)^{3}He (Ref. 41), and ^{6}Li(*p*,^{4}He)^{3}He (Ref. 41), respectively, which are consistent with the qualitative trend expected from Eq. (7). For D(D$^+$, *p*)^{3}H, the screening energy term $E_s(E)$ has also been extracted[23] from the difference between Eq. (2) and the measured values[38,39] of $\sigma_{exp}(E)$ for the D-D fusion reaction (1a) with D_2 gas targets. The extracted value[23] of $E_s(E) \approx 50$ eV is consistent with that expected for the 1*s* hydrogen electron with $E_s(E) \approx e^2/r_s \approx 27$ eV where $r_s \approx a_0$. For solid targets such as TiD and PdD, however, the electron screening range could be as small as a tenth of the Bohr radius, $r_s = a_0/10 \approx 0.05$ Å (Refs. 42, 43 and 44); hence the extracted values of $E_s(E)$ from the solid metal deuteride targets may be up to ten times [$E_s(E) \approx 300$ eV] larger than values [$E_s(E) \approx 50$ eV] (Ref. 23) extracted from a D_2 gas target.[38,39] Therefore, it is important to carry out precise measurements of $\sigma_{exp}(E)$ with improved accuracy for $E < 4$ keV(CM) with the deuterated metal targets. A nonequilibrium situation similar to that of electrolysis and G/S fusion experiments can be simulated by applying an external electric field (either dc or ac voltage) to the metal deuteride target.

The modified Coulomb penetration factor, $P_s(E)$, given by Eq. (6) is a general expression applicable to any screening electron density distribution $\rho_e(r)$ surrounding the positively charged hydrogen or deuterium nucleus. For a given screening electron distribution, the screening energy term, $E_s(E)$, in Eq. (4) is uniquely determined for each positive energy, $E > 0$, as in the case of a target consisting of atomic nuclei such as ^{3}He. For mobile deuterium atoms in deuterated metals (as in electrolysis experiments[3-18]), however, the screening electron density in a nonequilibrium situation is not known reliably from either theoretical calculations or experimental measurements. Existing theoretical models[45] for the screening electron density surrounding a positive charge embedded in a metal are based on zero-temperature linear response approximations for a degenerate electron gas, the validity of which has not been tested experimentally for these situations. An example of those models is the random-phase or Thomas-Fermi (TF) approximation. For the TF model, the screening electron density $\rho_{TF}(r)$ is given by Yukawa form, $\rho_{TF}(r) = -(Z_t e k_e^2/4\pi)\exp(-k_e r)/r$ leading to the TF screening potential,

$V_{TF}(r) = (Z_i Z_t e^2) e^{-k_e r} / r$, where $k_e^{-1} = (4k_F / \pi a_0)^{1/2}$ is the TF screening length, with k_F being the electron Fermi wave number.[45] The TF model has been used by Vaselli *et al.*[46] to describe the cold fusion process in metals. The adequacy of the linear response approximation[45] has not been investigated, and a reliable nonlinear theory at finite temperatures is yet to be developed and implemented for mobile deuterium (or hydrogen) atoms in solid metal lattices, liquids, or liquid metals.[42] The combined effect of electrons and mobile atoms may lead to a further reduction of the Coulomb barrier via a shorter coherent screening length[42-44] $r_s = k^{-1} = (k_e^2 + k_t^2)^{-1/2}$ in an effective screened potential, $V(r) = (Z_i Z_t e^2) \exp(-kr) / r$, where k_e^{-1} is the TF screening length and $k_t^{-1} = (k_B T / 4\pi e^2 n_t)^{1/2}$ is the mobile atom modification length with the target atom density, n_t. Ultimately, the validity of any theoretical model for $\rho_e(r)$ and the electron screening potential have to be tested by direct and/or indirect measurements. The cross-section measurements for reactions (1a), (1b), and other similar charged particle nuclear reactions at low energies should provide direct measurements of $E_s(E)$ and indirect measurements of $\rho_e(r)$ for deuterated solid (or liquid) targets in a nonequilibrium situation similar to that of the G/S fusion experiment with pulsed high dc voltage.

II.C Fusion Reaction Rates

Reaction rates, R_{mono}, for both reactions (1a) and (1b) for monoenergetic incident deuterons with kinetic energy E_i in the laboratory (LAB) frame are given by

$$R_{mono}(1a) = R_{mono}(1b) = \Phi P(E_i). \tag{8}$$

The value Φ is the deuterium flux incident on the target area A:

$$\Phi = n_i A \upsilon = (0.625 \times 10^{19}\ \mathrm{D}^+ / s) I, \tag{9}$$

where

I = current (A)

n_i = incident deuterium density

υ = deuterium velocity.

The value $P(E_i)$ is the probability for a deuteron to undergo a fusion reaction (1a), or (1b) while slowing down in the deuterated palladium layer, which can be written as

$$P(E_i) = 1 - \exp\left[-\int dx\, n_D\, \sigma(E_{DD})\right] \approx \int dx\, n_D \sigma(E_{DD})$$

$$= n_D \int_0^{E_i} dE_D \frac{1}{|dE_D / dx|} \sigma(E_{DD}). \tag{10}$$

Values E_D and E_{DD} are the deuteron kinetic energies in the LAB and CM frames, respectively, ($E_{DD} = E_D/2$). The stopping power[47] for $E_D \leq 12$ keV is given by

$$\frac{dE_D}{dx} = 3.70 \times 10^{-15}\, n_{Pd} \sqrt{E_D}\ \mathrm{eV \cdot cm^2} \tag{11}$$

for deuterium in palladium and

$$\frac{dE_D}{dx} = 0.89\times10^{-15}\, n_D \sqrt{E_D}\ \text{eV}\cdot\text{cm}^2 \tag{12}$$

for deuterium in deuterium. Therefore, the stopping power for deuterium in PdD is given by the sum of Eqs. (11) and (12),

$$\frac{dE_D}{dx} = 3.1\times10^{5}\sqrt{E_D}\ \text{keV/cm}\ , \tag{13}$$

for $n_{Pd} = 6.767 \times 10^{22}$ cm^{-3} and $n_D = n_{Pd}$. E_D in Eq. (13) is in units of kilo-electron-volts in the LAB frame.

If we use Eq. (13) and the conventional extrapolation formula for $\sigma(E)$ given by Eq. (2), the integration in Eq. (10) can be done analytically to yield the following expression for Eq. (8),

$$R_{mono}(1a) \approx R_{mono}(1b) = 1.04\times10^{-6}\,\Phi \exp\left(-44.40/\sqrt{E_i}\right), \tag{14}$$

where R_{mono} in measured in s^{-1} and E_i in kilo-electron-volts (LAB), assuming equal branching ratios for reactions (1a) and (1b).

For cold fusion experiments, the incident deuterium flux is not monoenergetic but has a velocity distribution as discussed previously at the beginning of this section. Therefore, the reaction rate, R_{mono}, given by Eq. (8) must be modified. The modified expression for the reaction rate, R_{calc}, which takes into account a velocity distribution, $f(\upsilon)$, is given by

$$R_{calc} = \left(\Phi/\bar{\upsilon}\right)\int f(\upsilon)\upsilon P(\upsilon)\, d\upsilon\ , \tag{15}$$

where the relative velocity v is related to E_D by $E_D = \frac{1}{2}M_D\upsilon^2$, and $P(\upsilon)$ is the probability of fusion reaction given by Eq. (10). The velocity distribution function, $f(\upsilon)$, is normalized to $\int f(\upsilon)d\upsilon = 1$ and $\bar{\upsilon} = \int \upsilon f(\upsilon) d\upsilon$.

To see whether D-D fusion in electrolysis or G/S fusion experiments occurs mainly in the surface layers of palladium, the range $\Delta x(E_i)$ of D^+ in PdD is calculated in the following. $\Delta x(E_i)$ can be obtained from Eq. (13) as

$$\Delta x(E_i) = \int dx = \int_0^{E_i}\left(\frac{dE}{dx}\right)^{-1} dE = 0.654\times10^{-5}\sqrt{E_i(\text{in keV})}\ \text{cm}\ , \tag{16}$$

which yields $\Delta x(E_i)$ = 20.4, 64.5, and 204 Å for E_i = 1, 10, and 100 eV, respectively. The range $\Delta x(E_i)$ of D^+ in D_2 gas is larger than that of D^+ in PdD. Since individual deuterium atoms in palladium are separated by ~ 2 Å, the D^+ penetrates into the first 10, 32, and 102 atomic layers from the surface of PdD when the incident D^+ energies (LAB) are 1, 10, and 100 eV, respectively. Therefore, D-D fusion takes place within the surface atomic layers of PdD and/or within the D_2 gas pockets outside the palladium metal surface in the G/S fusion experiment.

For order of magnitude estimates, the D-D fusion reaction rate, R_{calc}, Eq. (15) can be approximated as

$$R_{calc} \approx \left(\Phi/\bar{\upsilon}\right)\Delta x\,\Lambda(E) = \left(0.208\times10^{-12}\ s\right)\Phi\Lambda(E), \tag{17}$$

where Δx is an effective interaction thickness of the target given by Eq. (16) and $\Lambda(E)$ is given by

$$\Lambda(E) = n_D \int \sigma(\upsilon)\upsilon f(\upsilon) d\upsilon . \tag{18}$$

The precise form of the deuterium velocity distribution in the G/S fusion experiment[29] is not known at present. If $f(\upsilon)$ is assumed to be a Maxwell-Boltzmann velocity distribution with a cut-off for high velocity components, the D-D fusion rate, $\Lambda(E_0)(s^{-1}/D)$, is given by

$$\Lambda(E_0) = \frac{n_D (8/\pi)^{1/2}}{M^{1/2}(E_0)^{3/2}} \int_0^{E_c} \sigma(E) E \exp[-E/E_0] dE , \tag{19}$$

where the cross-section, $\sigma(E)$, is parameterized (E is in the CM frame) by Eq. (5) assuming nonresonant charge-particle reactions for reactions (1a) and (1b). E_c in Eq. (19) is the upper integration limit beyond which the high velocity components are cut off. Value E_0 in Eq. (19) is related to the average deuterium kinetic energy as $\overline{E}_{DD}(CM) = \left(\frac{3}{2}\right) E_0$ or $\overline{E}_D(LAB) = \frac{1}{2} M_D \overline{\upsilon}^2 = 3E_0$, where M_D is the deuteron rest mass and $\overline{\upsilon}$ is the average velocity of incident deuterium ions.

The fusion rates $\Lambda(E)$ for reactions (1a) and (1b) have been calculated[24] using Eq. (19) and Eq. (5) with the replacement of $E_s(E)$ in Eqs. (4) and (5) by a constant given by $E_s(E) = \tilde{E}_s = e^2/r_s$. The calculated results[24] are presented in Table 1 for parametric values of $\tilde{E}_s$ = 0, 1, 2, 4, 6 and $10e^2/a_0$ and $n_D = 6 \times 10^{22}$ cm^{-3}. The case of $\tilde{E}_s = 0$ in Table 1 corresponds to the conventional Gamow factor (no electron screening). The expected coherent screening length r_3 discussed in section II.B is $r_s = k^{-1} = (k_e^2 + k_D^2)^{-1/2} \approx k_D^{-1} = (k_B T / 4\pi e^2 n_D)^{1/2} \approx 0.049$ Å with $T = 300$ K and $n_D = 6 \times 10^{22}$ cm^{-3}. Recent elaborate calculations[42,44] also yield $r_s \geq 0.05$ Å, corresponding to $E_s \leq 10e^2/a_0 = 270$ eV. As can be seen from Table I and Fig. 2, the electron screening effect becomes larger at lower energies. To demonstrate the large effect of deuterium velocity distribution on the fusion rates, the calculated results[22,24] of $\Lambda(E_0) = n_D \sigma(E_0) \upsilon$ are shown in Table 2. As can be seen from Tables I and II, the effect of both velocity distribution and electron screening becomes significant at low energies.

Table I

Low-energy fusion rates $\Lambda(E_0)$

for Reaction (1a) or (1b) *

E_0 (eV)	$\tilde{E}_s$					
	0	1	2	4	6	10
10	-27.7	-26.5	-25.3	-23.0	-20.6	-16.1
20	-20.1	-19.5	-18.9	-17.7	-16.5	-14.2
30	-16.4	-16.0	-15.6	-14.8	-14.0	-12.2
40	-14.0	-13.7	-13.4	-12.9	-12.3	-11.1
50	-12.4	-12.2	-11.9	-11.4	-11.0	-10.0

* Assuming equal branching ratios calculated from Eq. (19) using $n_D = 6 \times 10^{22}$ cm^{-3} and modified Coulomb penetration factor [Eq. (4)] in which $E_s(E)$ is assumed to be a constant independent of E, i.e. $E_s(E) = \tilde{E}_s = e^2/r_s$, with a single parameter, r_s. The value $\tilde{E}_s = 0$ corresponds to the conventional Gamow factor. The rates are expressed as the $\log_{10}$ of $\Lambda(E_0)$ in s^{-1} /D. The quantity $\tilde{E}_s$ is given in units of $e^2/a_0 = 27.17$ eV with $a_0 = 0.53$ Å. The value E_0 is in CM reference frame, $E_0 = \frac{2}{3}E_{DD}$. Calculations of $\Lambda(E_0)$ with the upper integration limit $E_c \geq 1.0$ keV in Eq. (19) yield the same results.[22]

Table II

Calculated Results for Reaction (1a) or (1b)*

E (eV)	$\tilde{E}_s$					
	0	1	2	4	6	10
10	-127.7	-61.9	-44.9	-30.7	-23.9	-16.9
20	-87.7	-54.1	-41.3	-29.3	-23.2	-16.6
30	-70.1	-48.4	-38.4	-28.0	-22.4	-16.2
40	-59.6	-44.1	-35.9	-26.8	-21.7	-15.9
50	-52.5	-40.6	-33.7	-25.7	-21.1	-15.5

* Assuming equal branching ratios with a sharp (monoenergetic) distribution, $\Lambda(E) = n_D\sigma(E)\upsilon$. Taken from Refs. 22 and 24

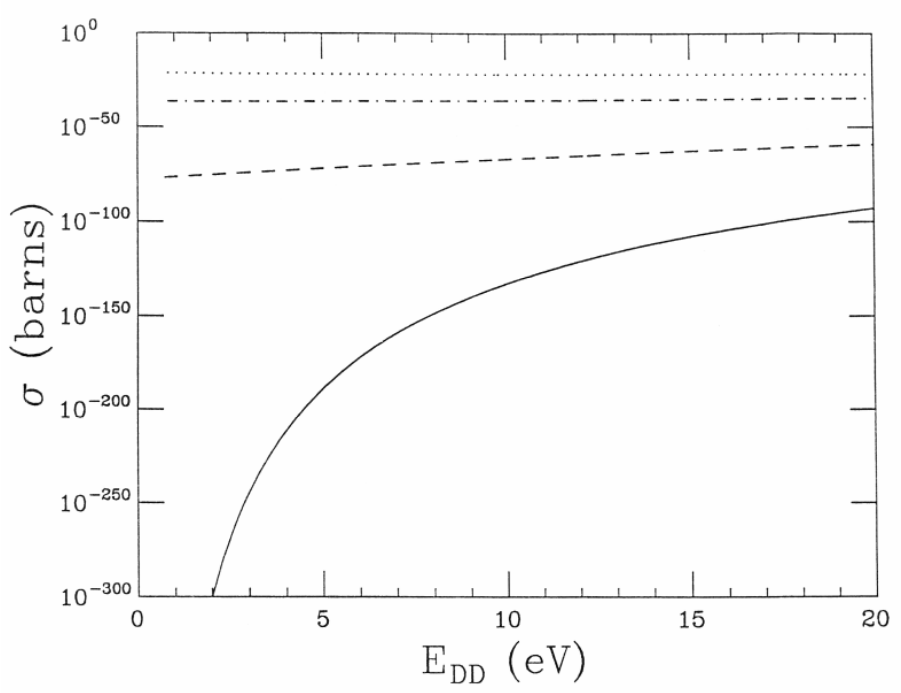

Fig. 2. The calculated cross-sections[24] $\sigma(E_{DD})$ for reactions (1a) and (1b), D(D,*p*)T and D(D,*n*)3He, for the CM energy, $E_{DD} < 20$ eV with $E_s(E) = \tilde{E}_s = 0, 1, 4, 10\ e^2/a_0$ using Eq. (5): $E^2/a_0 = 27.17$ eV with the Bohr radius, $a_0 = 0.53$ Å. The solid, dashed, dash-dotted, and dotted lines refer to the results of calculations using $\tilde{E}_s = 0, 1, 4$, and 10 e^2/a_0, respectively.

The expected upper limit of the D-D fusion rates inside the palladium surface for the case of the G/S fusion experiment by Claytor *et al.*[29] can be obtained from Eq. (14) with $E_i \leq 3$ keV as

$$R^T_{PdD}(1a)\ \left(\text{or}\ \ R^n_{PdD}(1b)\right) \lesssim 7.65\times10^{-18}\,\Phi = 48\ \ I_D\,(\text{A})\ \text{s}^{-1}, \tag{20}$$

where the net deuterium spark discharge current I_D (in amperes) generated in the D_2 gas pockets is not the same as the measured external current (< 0.5 amp.)[29] across the G/S fusion cell. The spark discharge current densities are known to be large ($\leq 10^6$A/cm^2)[32,33] corresponding to 0.625×10^{25} charge/s·cm^2, lasting ~ 10 μs. In the G/S fusion cells used by Claytor *et al.*,[29] the total volume of palladium layers is ~ 7 cm^3. If D_2 gas pockets with an average size of 10 μm occupies one seventh (~ 1 cm^3) of the total volume of ~ 7 cm^3 (a conservative estimate), there will be 10^9 D_2 gas pockets in the G/S cell. Since the deuteron density of D_2 gas at 10 atm. is ~ 6×10^{20} D/cm^3, each D_2 gas pocket contains ~ 6×10^{11} D. If one sixth of the ~ 6×10^{11} D in a single pocket (or 10^{20} D/cm^3) on average are accelerated during a spark discharge period of ~ 10 μs, the deuteron flux is $\Phi \approx 10^{20}$ D/10 μs = 10^{25} D/s, and the upper limit of R_{PdD} given by Eq. (20) is $R_{PdD} \approx 7.65 \times 10^7$ s^{-1} with $E_i \approx 3$ keV. At $E_i \approx 3$ keV, the electron screening effect is not important and may increase the upper limit [Eq. (20)] by less than one order of magnitude. The neutron production rate of $R^n_{exp}(1b) \approx 10^{-2}\ \text{s}^{-1}$ observed by Claytor *et al.*[29] is well below the upper limit given by Eq. (20), while their observed tritium production rate of $R^T_{exp}(1a) \approx 10^7\ \text{s}^{-1}$ will require a net deuteron flux Φ greater than 10^{26} D/s in Eq. (20).

With the flux value of $\Phi \approx 10^{25}$ D/s, the expected values of the D-D fusion rates for reaction (1a) and (1b) can be computed from Eq. (17) with $\Lambda(E_0)$ given in Table 1. When there is no electron screening (for conservative estimates with $\tilde{E}_s = 0$ in Table 1), the calculated values are

$R_{calc} = \left(0.208\times10^{-12}\,\mathrm{s}\right)\Phi\Lambda\left(E_0\right) = 2.08\times10^{-2}\,\mathrm{s}^{-1}$ and 0.832×10^{-1} s^{-1} for E_0 = 40 eV and E_0 = 50 eV, respectively. The observed value[29] of $R^{n}_{\mathrm{exp}}(1b) \approx 10^{-2}\,\mathrm{s}^{-1}$ is bracketed by the above calculated values, while the observed tritium production rate of $R^{T}_{\mathrm{exp}}(1a) \approx 10^{7}\,\mathrm{s}^{-1}$ will require a net flux $\Phi > 10^{25}$ D/s, or alternatively, a larger value of E_0 and/or an enhancement of the low-energy cross section.

Dramatic increases of the D-D fusion rates can be achieved if a higher pulsed dc voltage ($\leq$ 100 kV) is used. For E_i = 100 keV, Eq. (14) yields an upper limit of $R_{\mathrm{PdD}} \leq 1.23 \times 10^{-8}\,\Phi$, which is an increase of 10^9 from the upper limit of $7.65 \times 10^{-18}\,\Phi$ given by Eq. (20) for E_i = 3 keV. For an input power of $I_{cell}V_{cell}$ = (1 A) (100 kV) = 100 kW for a single G/S cell with E_i = 100 keV, $\Phi \geq 1.26 \times 10^{26}$ D/s is required to reach the break-even point, since a fusion rate of $R_{\mathrm{PdD}} \approx 1.55 \times 10^{18}$ s^{-1} is needed to produce the fusion energy output of 100 kW with 4.03 MeV = 6.45×10^{-13} J per reaction (1a). With the use of multiple cells or a larger cell with an improved design, the above break-even requirement for Φ can be made lower.

The above estimates of the D-D fusion rate in the palladium surface layers indicate that the surface fusion mechanism provides plausible explanations of the reproducible results of Claytor *et al.*,[29] and also of the nonreproducible positive results[3-18] and negative results[25-28] of electrolysis fusion experiments, in which it is difficult to maintain and control the total number and size of the D_2 gas bubbles. In contrast, the D_2 gas pockets in the G/S fusion device of Claytor *et al.*[29] are numerous ($\geq 10^6$), stable, and can be prefabricated. Furthermore, a very high pulsed dc voltage ($\leq$ 100 kV) can be used in the G/S fusion device as in the experiments of Claytor *et al.*,[29] while applicable dc voltages are very small (1 to 20 V) in electrolysis experiments,[3-18,25-28] The reaction cross-sections and fusion rates for reactions (1a) and (1b) from electrolysis experiments[3-18,25-28] therefore are expected to be substantially smaller than those from the G/S fusion experiments.[29]

II.D Anomalous Branching Ratios and Secondary Reactions

The observed branching ratio, $R^{T}_{\mathrm{exp}}(1a)/R^{n}_{\mathrm{exp}}(1b) \leq 10^9$ by Claytor *et al.*[29] and others[12,13] is contrary to the conventional assumption of nearly equal branching ratios expected from charge symmetry and charge independence of the nuclear force, and is yet to be explained theoretically if the experimental data are definitively confirmed.

After the incident deuteron penetrates through the Coulomb barrier to within an effective nuclear interaction range of 8 F (twice the deuteron radius), nuclear dynamics take over for this system of four nucleons. One possible explanation for the unequal rates is that there may be a broad resonance behavior in $\sigma(E)$ for reaction (1a) but not in $\sigma(E)$ for reaction (1b) at low energies. This is plausible since the final state Coulomb interaction is present for reaction (1a) but not for reaction (1b). If $\sigma(E)$ happens to have resonance behavior near $E \leq 100$ eV, the extrapolation may yield erroneous values for $\sigma(E \sim 100$ eV), since the nonresonant relation (2) or (4) is not applicable to resonance reactions. Therefore, it is very important to investigate theoretically the possibility of resonance behavior for $\sigma(E)$ near $E \leq 100$ eV, and also to measure $\sigma(E \leq 3$ keV) directly with precision experiments as suggested previously.[48]

Another possible explanation is that there may be resonances for the reaction D(2D,T)^{3}He at low energies. The three-body collision frequency is astronomically small in three-dimensional space in the case of conventional plasma fusion, but may become comparable to that of two-body

collisions[49] in the case of one-dimensional channeling, a process that occurs in ion implantation or in a similar situation as in G/S fusion.

An interesting possibility is that the anomalous branching ratio may be understood as an effect of the extension of Efimov's effect[50,51] to the four-nucleon system and the three-deuteron system. Efimov demonstrated a remarkable and hitherto unsuspected property of three-body systems by showing that if three nonrelativistic identical particles interact via short-range two-body potentials $gv(r)$, then as the coupling constant g increases to that value g_0 which can support a single two-body bound state at zero energy, the number of bound states of the three-particle system increases without limit, being roughly given by the formula $N \approx (1/\pi) ln(|a|/r_0)$, where a is the two-body scattering length (which becomes infinite whenever there is a zero-energy s-wave two-body bound state) and r_0 is the range of the potential $v(r)$. This implies that whenever there is a two-body bound state with zero binding energy, there are an infinite set of solutions of the three-body Schroedinger equation with E complex and very near zero.[52,53] Whether such states can be observable resonances or virtual states for four-nucleon and three-deuteron systems should be investigated in terms of (1) Efimov's effect for the 2-D system as a three-body system, (D+p+ n), (2) generalization of Efimov's effect to four-body systems, and (3) Efimov's effect for the 3-D system. An Efimov or Efimov-like effect is expected to be different between reactions D(D,p)T and D(D,n)^{3}He due to different final-state interactions. It also implies that a low-energy 3-D resonance may exist if a low-energy 2-D resonance exists.

At present, there are neither direct experimental measurements nor theoretical calculations of the branching ratio for reaction (1a) to reaction (1b) for $E \leq 3$ keV. One would expect the reaction rate of reaction (1a) to be larger than that of reaction (1b), since reaction (1b) involves a fusion of two protons to form ^{3}He while reaction (1a) does not fuse two protons but merely transfers a neutron from one deuteron to the other to form ^{3}H. Reliable theoretical calculations of the reaction cross-sections and branching ratio of reactions (1a) and (1b) are yet to be carried out based on nonrelativistic four-nucleon scattering theory[54] using nucleon-nucleon forces and the Coulomb interaction.

The tritium produced at the rate of $R^T_{\exp}(1a) \approx 10^7\ s^{-1}$ in the experiment of Claytor *et al.*[29] should have produced 14 MeV neutrons via the secondary reaction, T + D → ^{4}He(3.5 MeV) + n(14.1 MeV), which has an expected rate of $10^7 \times 10^{-5} \approx 10^2\ s^{-1}$, since the probability given by a relation similar to Eq. (10) is expected to be $P(E) \approx 10^{-5}$, unless tritium is produced from reaction (1a) with very low kinetic energies for some unexpected reason. In addition to the above secondary reaction, 3 MeV protons produced from reaction (1a) at the same rate as tritium should have produced de-excitation gamma rays (0.37 ~ 0.56 MeV)[28] from proton-induced Coulomb excitation of palladium isotopes. Future measurements of these secondary nuclear reactions can provide additional information for understanding the unexpectedly large value of the D-D fusion rate for reaction (1a).

III. OPTIMIZATION CONDITIONS FOR THE SURFACE FUSION MECHANISM

For the surface reaction mechanism for low-energy D-D fusion, the total fusion rate, R_{calc}, is given by Eq. (15), or approximately by Eq. (17). R_{calc} depends mainly on (a) the target deuterium density in the deuterated metal and in the D_2 gas pockets, (b) the incident deuterium flux, and (c) the kinetic energy (or velocity) of the incident deuterium ions. Therefore, quantities (a), (b), and

(c) must be maximized within the limitations imposed by a given experimental set-up for a G/S fusion device.

III.A Target Deuterium Density

In order to maximize the fusion rates, R_{calc}, the deuterium density, n_D, in Eq. (10) or Eq. (18), should be optimized and maintained at a maximum value inside the surface of the deuterated metal and in the D_2 gas pockets. High deuterium density in the metal is also needed to rapidly replace depleted D_2 molecules in the D_2 gas pockets by desorption:

1. Choice of the target metal is important for high n_D values; the metal should have a high value of deuterium solubility at a reasonably high temperature (100 ~ 500°C for practical energy generation).

2. High values of applied D_2 gas pressure should be helpful in maintaining high deuterium density in the metal and in the D_2 gas pockets.[55]

III.B Deuterium Flux

To maximize the fusion rate for a given experimental setup, the deuterium flux should be maximized by optimizing the net deuterium spark current.

1. A metal oxide coating of ~ 10 Å thickness on the metal surfaces is known to improve D-D fusion rates.[29] This procedure of oxidizing the metal surface may help to maintain the metal surface integrity including preservation of the asperities and a high deuteron surface density by preventing surface poisoning due to incident discharge currents.

2. It is important to use a pulsed dc voltage ($\leq$ 100 kV) source, since the deuterium ions are accelerated as spark currents inside the D_2 gas pockets due to the electric fields generated by the applied external voltage. The desirable dc voltage pulse duration is expected to be 1 to 10 μs since the spark current is known to reach a peak value within 1 μs and to decay to half-value in 10 to 30 μs.[32]

The duty cycle of the pulsed high dc voltage should be optimized by synchronizing it with an average recovery time during which the original gas density in the pockets is restored by D_2 gas diffusion and also by desorption from the deuterated metal after D_2 molecules are depleted by spark discharge and D-D fusion in the gas pockets.

3. The asperities on the surface of the deuterated metal which penetrate into D_2 gas pockets are useful in providing an efficient mechanism for accelerating the deuterium ions[23] and for producing the spark discharge current.[32,33] A means of optimizing this physical situation should be found.

4. The size d of the D_2 gas pocket and the D_2 gas pressure, p, should be optimized for attaining a maximum value of the incident deuterium flux, since the breakdown voltage beyond which the D_2 gas (an insulator) in the pocket becomes a conductor producing the D^+ current depends on d and p as a function of the product dp. (Refs. 32 and 33).

5. The total number of D_2 gas pockets and the surface area of the deuterated metal exposed to the D_2 gas pockets should be maximized to generate a maximum deuterium flux.

6. During spark discharge in the D_2 gas, electrons emitted from D_2 molecules and the metal surface tend to inhibit higher deuterium ion currents. Since the electron mass is much smaller

than the deuteron mass, electrons can be deflected to the sides away from the deuterium flux by an applied magnetic field of appropriate magnitude and direction. The deuterium flux can be enhanced by application of a pulsed magnetic field in synchronization with the pulsed dc voltage.

III.C Incident D^+ Kinetic Energy

Since the cross-section $\sigma(E)$, Eq. (2) or (5), increases rapidly as a function of increasing value of the incident deuterium kinetic energy,[22,24] the total fusion rate, R_{calc}, can be increased by raising the incident deuterium kinetic energy.

The use of pulsed high dc voltage should help to increase the high velocity component of the deuterium velocity distribution and the intensity of the spark current because the modulated voltage can be raised to a very high value (≤ 100 kV) without shorting out the experimental setup.

IV. SUMMARY AND CONCLUSIONS

It has been shown that the surface fusion mechanism can provide plausible explanations for both the reproducible results of the G/S fusion experiment of Claytor *et al.*[29] and the nonreproducible results of electrolysis fusion experiments.[3-18,25-28]

The D-D fusion rates, $R^T_{\exp}(1a) \approx 10^7\ \mathrm{s}^{-1}$ for reaction (1a) and especially $R^n_{\exp}(1b) \approx 10^{-2}\ \mathrm{s}^{-1}$ for reaction (1b), obtained by Claytor *et al.* from the G/S fusion experiments[29] are physically acceptable values in the context of the surface fusion mechanism.

The observed branching ratio, $R^T_{\exp}(1a)/R^n_{\exp}(1b) \leq 10^9$ is an unexpected result from the viewpoint of conventional nuclear theory based on the charge symmetry and charge independence of the nuclear force and may be due to resonance behavior in the cross-section favoring one channel over another at low energies. Therefore, it is very important to measure $\sigma(E \leq 3$ keV) for reactions (1a) and (1b) directly with precision experiments as previously suggested.[48] Historically, the frontier of nuclear physics has shifted from low energies (several kilo-electron-volts) to higher energies, bypassing the extreme low-energy regime (1 eV to 1 keV) partly due to experimental difficulties, and partly due to unjustified theoretical expectations that no new phenomena would be observed from a simple scaling of higher-energy results to the extremely low-energy regime. If the neutron and tritium production data are definitively confirmed in future experiments, a **new frontier** of nuclear physics research will open up in the extremely low-energy regime, which will also pose challenging problems in nuclear theory. Reliable theoretical calculations of the cross-sections for reactions (1a) and (1b) should be carried out in the context of nonrelativistic four-nucleon scattering theory which includes both the Coulomb interaction and nucleon-nucleon forces.

Finally, the nonreproducibility of the results of electrolysis fusion experiments[3-18,25-28] can be explained in terms of the surface fusion mechanism. Because of the inherent instability and problems associated with D_2 gas bubbles that form a thin gas layer, which can virtually cover the surface of the palladium cathode in electrolysis experiments, it is difficult to achieve appropriate conditions required for D-D fusion in electrolysis experiments, and to reproduce the same result consistently with the same and/or similar electrolysis cells.[3-18] The performance of the electrolysis fusion cells in achieving D-D fusion, therefore, is expected to be erratic and to

remain unreliable. Thus, the surface fusion mechanism can provide plausible explanations for the nonreproducibility of the claimed positive results[3-18] and for the numerous negative results[24-28] of electrolysis fusion experiments. In contrast to the shortcomings of electrolysis fusion cells, the D_2 gas pockets in a G/S fusion device are stable and physically controllable for each and every experiment; thus the G/S fusion device offers a more desirable and promising system in which experimental conditions for optimizing D-D fusion rates can be investigated reliably with reproducible results. The use of a high pulsed dc voltage of ~ 100 kV in the G/S fusion device may provide economic tritium production and may also lead to practical applications for large-scale economic power generation.

REFERENCES

1. Y. E. Kim, "Nuclear Theory Hypotheses for Cold Fusion," in the Proceedings of the NSF/EPPJ Workshop on Anomalous Effects in Deuterated Metals, Washington, D.C., October 16-18, 1989.
2. Y. E. Kim, "Fission-Induced Inertial Confinement Hot Fusion and Cold Fusion with Electrolysis," in *Laser Interaction and Related Plasma Phenomena,* Vol. 9 (H. Hora and G. H. Miley eds.), Plenum Press, New York (1990).
3. M. Fleischmann and S. Pons, "Electrochemically Induced Nuclear Fusion," J. Electroanal. Chem. **261,** 301 (1989); and errata **263,** 187 (1989).
4. M. Fleischmann, S. Pons, M. W. Anderson, L. J. Li, and M. Hawkins, "Calorimetry of the Palladium-Deuterium-Heavy Water System," J. Electroanal. Chem. **287,** 293 (1990).
5. S. Pons and M. Fleischmann, "Calorimetry of the Palladium-Deuterium System," in the Proceedings of the First Annual Conference on Cold Fusion, Salt Lake City, Utah, March 28-31, 1990, pp. 1-19.
6. A. J. Appleby, Y. J. Kim, O. J. Murphy, and S. Srinivasan, "Anomalous Calorimetric Results during Long-Term Evolution of Deuterium on Palladium from Alkaline Deuteroxide Electrolyte," in the Proceedings of the First Annual Conference on Cold Fusion, Salt Lake City, Utah, March 28-31, 1990, pp. 32-43.
7. M. Schreiber *et al.,* "Recent Measurements of Excess Energy Production in Electrochemical Cells Containing Heavy Water and Palladium," in the Proceedings of the First Annual Conference on Cold Fusion, Salt Lake City, Utah, March 28-31, 1990, pp. 44-56.
8. S. Guruswamy, J. G. Byrne, J. Li, and M. E. Wadsworth, "Metallurgical Aspects of the Electrochemical Loading of Palladium with Deuterium," to be published in the Proceedings of the NSF/EPRI Workshop on Anomalous Effects in Deuterated Metals, Washington, D.C., October 16-18, 1989.
9. M. C. H. McKubre *et al.,* "Calorimetry and Electrochemistry in the D/Pd System," in the Proceedings of the First Annual Conference on Cold Fusion, Salt Lake City, Utah, March 28-31, 1990, pp. 20-31.
10. R. Adzic, D. Jervasio, I. Bae, B. Cahn, and E. Yeager, "Investigation of Phenomena Related to D_2O Electrolysis at a Palladium Cathode," in the Proceedings of the First Annual Conference on Cold Fusion, Salt Lake City, Utah, March 28-31, 1990, pp. 261-271.
11. S. E. Jones *et al.,* "Observation of Cold Nuclear Fusion in Condensed Matter," Nature **338**, 737 (1989).
12. P. K. Iyengar *et al.,* "Bhabha Atomic Research Centre Studies in Cold Fusion," Fusion Technology 18, 32 (1990).

13. N. J. C. Packham, K. L. Wolf, J. C. Wass, R. C. Kainthala, and J. O. M. Bockris, "Production of Tritium from D_2O Electrolysis at a Palladium Cathode," J. Electroanal. Chem. 270, 451-458 (1989).
14. D. Gozzi, P. L. Cignini, L. Petrucci, M. Tomellini, and G. De Maria, "Evidence for Associated Heat Generation and Nuclear Products Release in Palladium Heavy-Water Electrolysis," Nuovo Cimento 130A, 143-154 (1989)
15. E. Storms and C. Talcott, "A Study of Electrolytic Tritium Production," in the Proceedings of the First Annual Conference on Cold Fusion, Salt Lake City, Utah, March 28-31, 1990, pp. 149-163.
16. C. D. Scott, J. E. Mrochek, T. C. Scott, G. E. Michaels, E. Newman, and M. Petek, "Measurement of Excess Heat and Apparent Coincident Increases in the Neutron and Gamma-Ray Count Rates during the Electrolysis of Heavy Water," Fusion Technology **18**, 103 (1990).
17. C. Sanchez, J. Sevila, B. Escarpiz, F. J. Fernandez, and J. Canizares, Solid State Comm. **17**, 1039 (1989).
18. Y. Arata and Y.-C. Zhang, "Achievement of An Intense Cold Fusion Reaction," Nuclear Fusion Research **62**, 398 (November 1989, in Japanese); Fusion Technology **18**, 95 (1990).
19. S. E. Koonin and M. Nauenberg, "Calculated Fusion Rate in Isotopic Hydrogen Molecules," Nature **339,** 690 (1989).
20. A. J. Leggett and G. Baym, "Exact Upper Bound on Barrier Penetration Probabilities in Many-Body Systems: Application to Cold Fusion," Phys. Rev. Lett. **63**, 191 (1989).
21. K. Langanke, H. J. Assenbaum, and C. Rolfs, "Screening Corrections in Cold Deuterium Fusion Rates," Z. Phys. A. Atomic Nuclei **333,** 317 (1989).
22. R. A. Rice, G. S. Chulick, Y. E. Kim, and Jin-Hee Yoon, "The Role of Velocity Distribution in Cold Deuterium-Deuterium Fusion," Fusion Technology **18**, 147 (1990).
23. Y. E. Kim, "Surface Reaction Mechanism and Lepton Screening for Cold Fusion with Electrolysis," in the Proceedings of the First Annual Conference on Cold Fusion, Salt Lake City, Utah, March 28-31, 1990, pp. 194-201.
24. R. A. Rice, G. S. Chulick, and Y. E. Kim, "The Effect of Velocity Distribution and Electron Screening on Cold Fusion," in the Proceedings of the First Annual Conference on Cold Fusion, Salt Lake City, Utah, March 28-31, 1990, pp. **185-**193.
25. M. Gai *et al.*, "Upper Limits on Neutron and 7-Ray Emission from Cold Fusion," Nature **340,** 29 (1989).
26. N. S. Lewis *et al.*, "Searches for Low-Temperature Nuclear Fusion of Deuterium in Palladium," Nature **340,** 525 (1989).
27. D. E. Williams *et al.*, "Upper Bounds on Cold Fusion in Electrolysis Cells," Nature **342,** 375 (1989).
28. M. H. Salamon *et al.*, "Limits on the Emission of Neutrons, γ-Rays, Electrons, and Protons from Pons/Fleischmann Electrolysis Cells," Nature **344**, 401 (1990).
29. T. N. Claytor, P. A. Seeger, R. K. Rohwer, D. G. Tuggle, and W. R. Dotty, "Tritium and Neutron Measurements of a Solid State Cell," Los Alamos National Laboratory Reprint LA-UR-89-39-46, to be published in the Proceedings of the NSF/EPRI Workshop on Anomalous Effects in Deuterated Metals, Washington, D.C., October 16-18, 1989.
30. A. Sieverts and W. Danz, "Die Loslichkeit von Deuterium und von Wasserstoff in festem Palladium. II," Z. Physik. Chem. (B) **34**, 158 (1936); **38**, 46 (1937).

31. M. Rabinowitz and D. H. Worledge, "An Analysis of Cold and Lukewarm Fusion," Fusion Technology **17**, 344 (1990).
32. J. M. Meek and J. D. Craggs, *Electrical Breakdown of Gases,* Oxford University Press, London (1953), Chapter 10.
33. F. Llewellyn-Jones, *Ionization and Breakdown in Gases,* John Wiley and Sons, Inc. (1957).
34. G. H. Lin, R. C. Kainthala, N. J. C. Packham, and J. O'M. Bockris, "Electrochemical Fusion: A Mechanism Speculation," J, Electroanal. Chem. **280,** 207 (1990).
35. H. Hora, L. Cicchitelli, G. H. Miley, M. Ragheb, A. Scharmann, and W. Scheid, "Plasma and Surface Tension Model for Explaining the Surface Effect of Tritium Generation at Cold fusion," Nuovo Cimento D **12**, 393 (1990).
36. P. H. Handel, "Reformulation of the Cold Fusion Problem: Heterogeneous Nucleation—A Likely Cause of the Irreproducibility and Intermittency of Cold Fusion Observations," in the Proceedings of the First Annual Conference on Cold Fusion, Salt Lake City, Utah, March 28-31, 1990, pp. 288-294.
37. W. A. Fowler, G. R. Caughlan, and B. A. Zimmermann, "Thermonuclear Reaction Rates," Ann. Rev. Astr. Astrophys. 5, 525 (1967); "Thermonuclear Reaction Rates II," **13**, 69 (1975).
38. A. von Engel and C. C. Goodyear, "Fusion Cross-Section Measurements with Deuterons of Low Energies," Proc. Roy. Soc. A **264,** 445 (1961).
39. A. Krauss, H. W. Becker, H. P. Trautvetter, and C. Rolfs, "Low-Energy Fusion Cross-Sections of D + D and D+^{3}He Reactions," Nucl. Phys. **465,** 150 (1961).
40. S. Engstler, A. Krauss, K. Neldner, C. Rolfs, and U. Schroder, "Effects of Electron Screening on the ^{3}He(d,p)^{4}He Low-Energy Cross Sections," Phys. Lett. B **202,** 179 (1988).
41. U. Schroder, S. Engstler, A. Krauss, K. Neldner, C. Rolfs, and E. Somor-jai, "Search for Electron Screening of Nuclear Reactions at Sub-Coulomb-Energies," Nuclear Instr. and Meth. B **40/41,** 466 (1989).
42. H. Takahashi, "Quantum Theory of Correlation Functions for Liquid Metals and Normal Liquids in the Zero Sound Wave Range," Physica **51,** 333 (1971); "Dynamical Screening of Potential by Mobile Deuteron and Fusion Rate of Accelerated Deuteron in Pd D_x," J. of Fusion Energy **9**, 441 (1990).
43. S. N. Vaidya and Y. S. Mayya, "Theory of Screening-Enhanced D-D Fusion in Metals," Jap. J. Appl. Phys. **28**, L2258 (1989).
44. K. B. Whaley "Boson Enhancement of Finite-Temperature Coherent Dynamics for Deuterium in Metals" Phys. Rev. B **41,** 3473 (1990).
45. A. Fetter and J. D. Walecka, *Quantum Theory of Many-Particle Systems,* McGraw-Hill (1970).
46. M. Vaselli, M. A. Harith, V. Palleschi, G. Salvetti, and D. P. Singh, "Screening Effect of Impurities in Metals: a Possible Explanation of the Process of Cold Nuclear Fusion," Nuovo Cimento D **12,** 927 (1989).
47. H. H. Anderson and J. F. Ziegler, *Hydrogen Stopping Powers and Ranges in All Elements,* Pergamon Press, New York (1977).
48. Y. E. Kim, "Cross-Sections for Cold Deuterium-Deuterium Fusion," Fusion Technology **17**, 507 (1990).
49. M. Rabinowitz, "High Temperature Superconductivity and Cold Fusion," Mod. Phys. Lett. B **4**, 233 (1990); private communication.
50. V. Efimov, "Energy Levels Arising from Resonant Two-Body Forces in a Three-Body System," Phys. Lett. **33B**, 563 (1970).

51. V. Efimov, “Weakly-Bound States of Three Resonantly-Interacting Particles,” Yad. Fiz. **12**, 1080 (1970) [Sov. J. of Nucl. Phys. 12, 589 (1971)].
52. R. D. Amado and J. V. Noble, “A New Pathology of Three-Particle Systems,” Phys. Lett. **35B**, 25 (1971).
53. R. D. Amado and J. V. Noble, “Efimov’s Effect: A New Pathology of Three-Particle Systems. II,” Phys. Rev. D **5**, 1992 (1972).
54. O. A. Yakubovsky, “On the Integral Equations in the Theory of *N* Particle Scattering,” Yad. Fiz. 5, 1312 (1967) [Sov. J. Nucl. Phys. **5**, 937 (1967)]; P. Grassberger and W. Sandhas, “Systematical Treatment of Non-Relativistic *N*-Particle Scattering Problem,” Nucl. Phys. B **2**, 181 (1967).
55. W. M. Mueller, J. B. Blackledge, and G. G. Libowitz, *Metal Hydrides,* Academic Press, New York (1968)